Thesis

Diagnostic value of TOF-^{18}F-FDG PET/CT in patients with benign pancreatic lesions – a retrospective study

submitted by

Bashar Hanna

for academic degree of

Doktor der gesamten Heilkunde

(Dr. med. univ.)

at the

Medical University of Graz

executed at the

Department of Radiology

Division of Nuclear Medicine

under the supervision of

Univ. FÄ Dr.in med. univ. Susanne Stanzel

Univ.-Prof. Dr.in med. univ. Reingard Aigner

Univ. FÄ Dr.in med. univ. Tina Nazerani-Zemann

Graz, 06.09.2024

Declaration of Academic Integrity

I declare on my honor that I have written this thesis independently and without outside help, that I have not used any sources other than those indicated, and that I have marked the passages taken verbatim or in substance from the sources used as such.

Graz, 06.09.2024 *Bashar Hanna eh*

Danksagungen

An dieser Stelle möchte ich meinen tiefsten Dank Frau Univ. FÄ Dr.in Susanne Stanzel für ihre ununterbrochene Unterstützung und Geduld über den gesamten Zeitraum der Erstellung meiner Diplomarbeit aussprechen. Eine bessere Betreuerin könnte ich mir nicht wünschen. Vielen Dank!

Bei meinen weiteren Betreuerinnen, Univ.-Prof.in Dr.in Reingard M. Aigner und Dr.in Tina Nazerani-Zemann möchte ich mich auch bedanken.

Mein Dank gilt auch besonders meiner Familie: Meinem Vater Masoun Hanna, meiner Mutter Geida Kerro, meinem Bruder Kinan und meiner Schwester Nancy. Ihr habt mich tagtäglich durch das ganze Studium und bei jedem Schritt in meinem Leben begleitet und bei jeder Hürde unterstützt. Euer Glaube an mich und eure ständige Ermutigung haben das alles ermöglicht.

Zu guter Letzt möchte ich mich bei meinen Freunden für die schönen Erinnerungen und für jeden Rat bedanken. Eure Unterstützung hat mir geholfen, in schwierigen Phasen durchzuhalten und stressige Situationen zu bewältigen.

Zusammenfassung

Fragestellung

Das primäre Ziel ist es zu überprüfen, ob der Einsatz des Time-of-Flight (TOF) Rekonstruktionsalgorithmus bei der ^{18}F-FDG PET/CT einen diagnostischen Benefit im Vergleich zur Standard-^{18}F-FDG PET/CT (ohne TOF) bei benignen Pankreasläsionen hat. Die sekundären Ziele umfassen die Evaluierung des Nutzens von TOF im Rahmen der ^{18}F-FDG PET/CT spezifisch bei Pankreasläsionen kleiner als 3 cm im Vergleich zur Standard-^{18}F-FDG PET/CT sowie der Korrelation zwischen der regionalen Speicherintensität und spezifischen Laborparametern (Leukozyten, CRP, Amylase, Lipase und LDH).

Methoden

In diese retrospektive Studie wurden 31 Patient*innen mit histologisch gesicherten gutartigen Pankreasläsionen und durchgeführter Zwei-Phasen ^{18}F-FDG PET/CT mit Aufnahmen 30 und 90 Min. p.i. und diagnostischem CT des Oberbauches eingeschlossen.
Die Früh- und Spätaufnahmen mit und ohne TOF wurden qualitativ und quantitativ miteinander verglichen und analysiert. Die qualitative Analyse erfolgte durch die visuelle Beurteilung der PET/CT-Aufnahmen. Die quantitative Beurteilung wurde mithilfe der Messung des maximalen Tracer-Uptakes (SUVmax) in den Früh- und Spätaufnahmen mit und ohne TOF und des Volumens in cm^3 der Läsionen durchgeführt. Die ermittelten SUVmax-Werte wurden anschließend mit den vorhandenen o.g. Laborparametern verglichen.

Ergebnisse

Von allen 31 Pankreasläsionen konnten mithilfe TOF 18 und ohne TOF 13 richtig als benigne identifiziert werden. Somit betrug die Effektivität mit TOF 58,06% (18/31) und 41,94% (13/31) ohne TOF (p= 0,112). Dabei betrug die Sensitivität 70,97% mit und 74,19% ohne TOF (p= 1,00). Von den 31 Läsionen waren ohne TOF 10 Läsionen und mit TOF 4 Läsionen nicht beurteilbar. Von den 28 Frühaufnahmen wurden mit TOF 19 und ohne TOF 15 Läsionen als benigne identifiziert. In den Spätaufnahmen wurden mit TOF 16 und ohne TOF 13 Läsionen als benigne beurteilt.
Die mittlere Läsionsgröße ± STABW betrug 2,71 ± 2,37 cm. Von den 21/31 Läsionen kleiner als 3 cm wurden mit TOF 12 und ohne TOF 9 Läsionen als benigne bewertet. Damit betrug die Effektivität mit TOF 57,14% (12/21) und 42,86% (9/21) ohne TOF (p=

0,261). Die Sensitivität betrug hingegen 71,43% mit TOF und 76,19% ohne TOF (p= 1,00) bei Läsionen kleiner als 3 cm. Von den 21 Läsionen waren 3 mit TOF und 7 ohne TOF nicht beurteilbar.

In den Früh- und Spätaufnahmen waren die SUVmax-Werte beim Einsatz von TOF signifikant höher im Vergleich mit den Werten ohne TOF (p= 0,002 bzw. p< 0,001).

Zwischen Lipase und SUVmax der Frühaufnahmen mit und ohne TOF sowie zwischen Amylase und SUVmax der Frühaufnahmen mit TOF konnte eine signifikante Korrelation gefunden werden. Zusätzlich ließ sich eine signifikante Korrelation zwischen CRP und SUVmax der Spätaufnahmen mit und ohne TOF feststellen.

Schlussfolgerung

Mit TOF konnte die Diagnoserate von benignen Pankreasläsionen um 16,1% verbessert werden im Vergleich zur Standard-Methode ohne TOF. Mithilfe TOF konnten somit mehr und insbesondere kleine (< 3 cm) Läsionen richtig als benigne klassifiziert werden, wenn auch keine statistisch signifikante Verbesserung der Diagnoserate erzielt wurde. Außerdem zeigte sich eine statistisch signifikante Korrelation zwischen dem SUVmax und dem Laborparametern Amylase, Lipase und CRP, was die erschwerte Unterscheidbarkeit entzündlicher von malignen Pankreaserkrankungen in der ^{18}F-FDG PET/CT erklärt. Daher sollten Patient*innen mit akuter oder chronischer Pankreatitis und erhöhten Amylase-, Lipase- oder CRP-Werten von der ^{18}F-FDG PET/CT-Untersuchung ausgeschlossen werden.

Abstract

Objectives of the Study

The primary objective is to examine if can the Time-of-Flight (TOF) reconstruction algorithm brings a diagnostic benefit in ^{18}F-FDG PET/CT compared to standard ^{18}F-FDG PET/CT (without TOF) in the evaluation of histologically confirmed benign pancreatic lesions. The secondary objectives include evaluating TOF in ^{18}F-FDG PET/CT in comparison with standard imaging without TOF particularly for pancreatic lesions smaller than 3 cm and the analysis of the correlation between the maximum tracer uptake (SUVmax) and specific laboratory parameters (leukocytes, CRP, amylase, lipase and LDH).

Methods

Thirty-one patients with histologically confirmed benign pancreatic lesions and performed dual phase (DP) ^{18}F-FDG PET/CT with imaging 30 and 90 min p.i. and diagnostic CT of the upper abdomen were included in this retrospective study.

The early and delayed scans with and without TOF were analyzed and compared with each other qualitatively and quantitatively. The qualitative analysis was made by visual assessment of the PET/CT scans. The quantitative analysis was performed through measuring the SUVmax in early and delayed scans with and without TOF and the volume of the lesions in cm^3. The determined SUVmax values were compared subsequently with the available laboratory markers (leukocytes, CRP, amylase, lipase, LDH).

Results

Out of all 31 pancreatic lesions 18 were correctly evaluated as benign with and 13 without TOF reconstruction. Thus, the effectivity with TOF was 58.06% (18/31) and 41.94% (13/31) without TOF (p= 0.112). The sensitivity was 70.97% with and 74.19% without TOF (p= 1.00). Out of the 31 scans 10 were not assessable without TOF and 4 with TOF. Out of the 28 early scans 19 were evaluated as benign with TOF and 15 without TOF. In delayed scans 16 lesions were evaluated as benign with TOF and 13 without TOF.

The mean ± SD lesion size was 2.71 ± 2.37 cm. Of 21/31 lesions measured smaller than 3 cm with TOF 12 and without TOF 9 lesions were evaluated as benign. Consequently, the effectivity was with and without TOF 57.14% (12/21) and 42.86% (9/21), respectively, (p= 0.261). By contrast, the sensitivity came to 71.43% and 76.19% with and without TOF,

respectively (p= 1.00). Three out of the 21 lesions were not assessable with TOF versus seven without TOF.

With TOF reconstruction, in early and delayed imaging the SUVmax values were significantly higher compared with SUVmax values without TOF ($p = 0.002$ and $p < 0.001$, respectively).

Between lipase and SUVmax in early imaging with and without TOF as well as between amylase and solely SUVmax with TOF in early imaging a significant correlation was spotted. Additionally, a significant correlation was found between CRP and SUVmax in delayed imaging with and without TOF.

Conclusion

With TOF reconstruction, the diagnosis rate of benign pancreatic lesions was improved by 16.1% compared to standard imaging without TOF. Thus, with TOF, more and particularly small (< 3 cm) lesions could be identified as benign, although no statistically significant improvement in the diagnosis rate was achieved. Furthermore, the SUVmax and the laboratory parameters amylase, lipase and CRP correlated significantly, explaining the difficulty in differentiation between inflammatory and malignant pancreatic lesions in ^{18}F-FDG PET/CT. Consequently, patients with acute or chronic pancreatitis and elevated amylase, lipase or CRP values should be excluded from ^{18}F-FDG PET/CT.

Table of Contents

Glossary and abbreviations

BGO ..... *bismuth germinate*

Bq ..... *Becquerel*

CA ..... *contrast agent*

cm ..... *centimeter*

E1 ..... *elastase 1*

^{18}F *fluorine-18*

FDG ..... *fluordesoxyglucose*

GFR ..... *glomerular filtration rate*

GORD ..... *gastro-oesophageal reflux disease*

GSO ..... *gadolinium oxyorthosilicate*

IPMN ..... *intraductal papillary-mucinous neoplasm*

L ..... *liter*

LDH ..... *lactate dehydrogenase*

LOR ..... *line-of-response*

LSO ..... *lutetium orthosilicate*

LVB ..... *lumbar vertebral body*

LYSO ..... *lutetium yttrium oxyorthosilicate*

MBq ..... *megabecquerel*

MCN ..... *mucinous cystic neoplasms*

MeV ..... *megaelectronvolt*

mm ..... *millimeter*

MRCP ..... *magnetic resonance cholangiopancreatography*

MRI ..... *magnetic resonance imaging*

^{20}Ne *neon-20*

NET ..... *neuroendocrine tumors*

^{18}O *oxygen-18*

o.g. ..... *oben genannt*

p.i. ..... *post injectionem*

PET ..... *positron emission tomography*

SD ..... *standard deviation*

SPECT ..... *single-photon emission computed tomography*

SPSS ..... *Statistical Package for the Social Sciences*

STABW ..... *Standardabweichung*

SUV ..... *standardized uptake value*

SUVmax ..... *maximal standardized uptake value*

™ ..... *trademark*

TOF..... *time-of-flight*

TSH..... *thyroid-stimulating hormone*

VOI ..... *volume of interest*

WHO..... *World Health Organization*

List of figures

List of tables

1 Introduction

1.1 Pancreas

1.1.1 Anatomy

The pancreas is an organ of the digestive system, which is (secondary) retroperitoneal. It lies as an elongated organ across the upper abdomen and, for the most part, in the epigastric region. It can be anatomically divided into four sections: Head (caput), uncinated process, body (corpus) and tail (cauda). The body of the pancreas is mainly located at the height of the 1. lumbar vertebral body (LVB I) and lies on the right side in the concave duodenal sweep, the head of the pancreas extends to LVB II. The tail reaches in the left upper abdomen near the spleen [1]. The pancreas is 13-18 cm long and weighs 70-80 g.

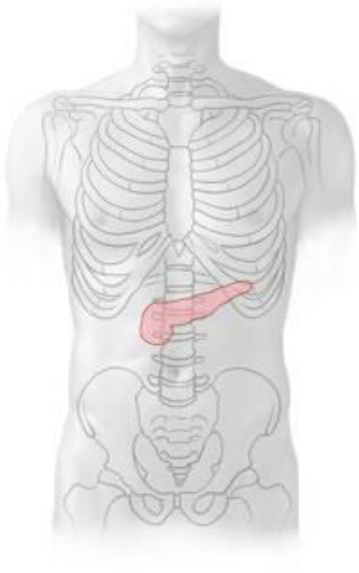

Figure 1 Location of the pancreas [1]

The main pancreatic duct (ductus pancreaticus) has a diameter of 2 mm, runs through the whole pancreas, and opens into the duodenum through the major duodenal papilla (papilla of Vateri) along with the common bile duct (ductus choledochus) [2].

The arterial blood supply of the pancreas is given by many arteries:

- anterior and posterior branches of the superior pancreaticoduodenal artery (originating from the gastroduodenal artery)

- inferior pancreaticoduodenal artery (originating from the superior mesenteric artery)

- dorsal pancreatic artery (origination from the splenic artery)

- greater pancreatic artery (originating from the splenic artery)

Blood from the body and tail of the pancreas drains through many small veins into the splenic vein, which runs in a tunnel in the posterior surface of the pancreas and drains into the portal vein. The head of the pancreas drains through the pancreaticoduodenal veins into the superior mesenteric vein, which drains into the portal vein as well [2].

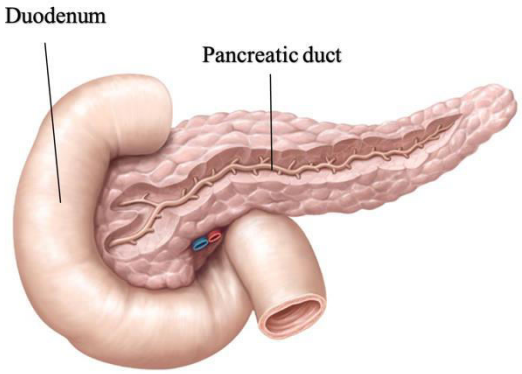

Figure 2 Location and course of the pancreatic duct [1]

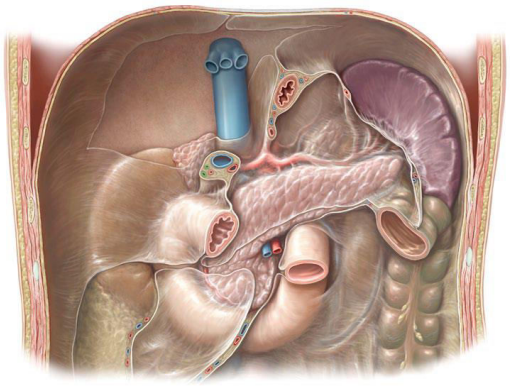

Figure 3 Pancreas in situ [1]

1.1.2 Physiology

Histologically, the pancreas consists of endocrine as well as exocrine gland tissue. The exocrine pancreas makes up to 98% of the organ's mass. It produces 1,5-2 L of pancreas juice, which contains bicarbonate and digestive enzymes to break down proteins, lipids, carbohydrates, and nucleic acids. The secreted enzymes are inactive proenzymes, which are activated by trypsin in the duodenum. The endocrine pancreas consists of islets of Langerhans, which comprise four different cell types that produce insulin, glucagon, somatostatin, and pancreatic polypeptide. Insulin and glucagon regulate blood glucose levels by increasing (glucagon induces the release of glucose from the liver) or decreasing (insulin induces uptake of glucose in muscle and fat cells) blood glucose concentration. A reduced insulin secretion or high insulin resistance in periphery cells lead to the metabolic disorder diabetes mellitus type I or II, respectively [1][2].

1.1.3 Pathology

1.1.3.1 Benign tumors of the pancreas

The World Health Organization (WHO) classifies benign tumors of the exocrine pancreas in [3]:

I. Serous cystic neoplasms of the pancreas
II. Mucinous cystic neoplasms of the pancreas
III. Intraductal papillary-mucinous neoplasms of the pancreas (IPMN)
IV. Neuroendocrine tumors (NET)

I. Serous cystic neoplasms of the pancreas:

Serous cystic tumors of the pancreas are predominantly benign tumors and rarely malignant (serous cystadenocarcinoma). Serous cystadenoma is the most common benign cystic neoplasm (30% of cystic tumors). It exhibits mostly more than five cysts that measure less than 2 cm for the most part in the body and tail of the pancreas [3] [5].

Approximately two third of the patients with serous cystic neoplasms show no symptoms. Around one third of the patients present with several symptoms due to the obstructive nature of the tumor: emesis, nausea, pain in the abdomen and back, diabetes mellitus and loss of weight. The mass can also be palpable at clinical presentation [6].

The diagnosis of serous cystic neoplasms consists in abdominal imaging. In computed tomography (CT) the neoplasms present with clearly defined borders and are multilocular. Nearly one third of the findings in CT show a central scar and a sunburst calcification. The neoplasms are hyperintense and hypointense in T2- and T1-weighted MRI images, respectively. On endoscopic ultrasound, they appear echogenic with multiple cysts and a typical honeycomb pattern [6].

II. Mucinous cystic neoplasms (MCN) of the pancreas

Mucinous cystic neoplasm (or mucinous cystadenoma) is defined as a septated mucin-producing, cyst-forming epithelial neoplasm of the pancreas with ovarian-type stroma. Mucinous cystadenoma affects almost only women and occurs predominantly in the body and tail of the pancreas. In imaging, small neoplasms less than 3 cm are discovered

incidentally, whereas patients with larger neoplasms present with symptoms due to compressing bordering organs. Imaging findings of mucinous cystic neoplasms show solitary as well as multilocular lesions with an average size of 7-8 cm. The cysts are surrounded by a thick fibrous wall [5] [11].

III. Intraductal papillary-mucinous neoplasms of the pancreas (IPMN):

Intraductal papillary-mucinous neoplasms are mucin-producing tumors deriving from the main pancreatic duct (ductus pancreaticus). This heterogenic category of pancreatic lesions arises predominantly in pancreatic ducts and can develop into invasive malignant tumors [4].

IPMNs can be divided into three groups [3]:

i. Intraductal papillary-mucinous adenoma with low-grade dysplasia
ii. Borderline intraductal papillary-mucinous neoplasms with moderate dysplasia
iii. Intraductal papillary-mucinous carcinoma with high-grade dysplasia
    - Non-invasive
    - Invasive (papillary-mucinous carcinoma)

IPMNs lead to a variety of unspecific clinical symptoms, which encompass recurrent pain in the upper abdomen and dilatation of the pancreatic duct system. These symptoms are caused by high mucin production and hence result in recurrent acute or chronic pancreatitis [5]. Furthermore, most patients with IPMNs may present with loss of weight, jaundice and diabetes mellitus. On the other hand, a few patients show none of the beforementioned symptoms [3].

The diagnosis of IPMNs is usually performed using endoscopic retrograde cholangiopancreatography (ERCP), magnetic resonance cholangiopancreatography (MRCP) or endoscopic ultrasound (EUS). A histological or cytological examination of the biopsy specimen of the lesion delivers further evidence for the presence of IPMNs. By surgical resection of the lesion and ensuing comprehensive histological examination of the resectate a certain diagnosis of an IPMN can be possible [3] [5].

IV. Neuroendocrine tumors (NET)

Neuroendocrine tumors represent approximately 2-5% of total pancreatic tumors. They are divided into two major groups depending on their hormone hypersecretion:

- Functional NETs
- Non-functional NETs

Due to the hypersecretion of specific hormones (e.g. insulin, gastrin, glucagon, etc.) functional NETs cause characteristic symptoms according to the particular hormone level elevation [7]. Hence, an insulinoma results from uncontrolled production of insulin in hypoglycemia, which can, in turn, lead to autonomic and neuroglycopenic symptoms [8], whereas a gastrinoma causes duodenal ulcers and gastro-oesophageal reflux disease (GORD) by inappropriate high secretion of gastrin [9].

Non-functional NETs don't result in syndromes due to hormone hypersecretion; however, they are discovered incidentally by clinical examinations or in case of noticeable mass growth [10]. Both functional and non-functional NETs have the potential to develop into malignant tumors depending on their proliferative activity (Ki-67 proliferation index). Low-grade G1 (well-differentiated) pancreatic NETs are tumors with low proliferative activity (Ki-67 < 3%), whereas tumors with higher proliferative activity are graded as G2 (moderately differentiated, Ki-67 3-20%) and G3 (poorly differentiated, Ki-67 >20%) [7][10]. The Types of benign pancreatic tumors are listed in Table 1.

Table 1 Types of benign tumors of the pancreas

Type	histology	Localization	epidemiology
Serous cystic neoplasms	cuboidal to flat epithelial cells	50-75% in body and tail	70% in women
Mucinous cystic neoplasms (MCN)	columnar, mucin-producing cells	body or tail	98% in women
IPMN	gastral-, intestinal- and pancreatobiliary-type epithelium	head	M:F (main duct-type IPMN) 3:1 (Japan and South Korea) 1.1:1 (USA)
NET	Cells of islets of Langerhans	All parts of the pancreas	Insulinoma: F > M

1.1.3.2 Pancreatitis

Pancreatitis is a collective term for quite often pancreatic diseases in which an autodigestion of the gland tissue dominates, and depending on the progression, a fibro-destructive pattern leads to exocrine pancreatic insufficiency [12]. Based on clinical and morphological criteria, pancreatitis is divided into acute and chronic pancreatitis [13].

I. Acute pancreatitis

Acute pancreatitis is a necrotizing inflammation of the pancreas as a consequence of an abrupt occurring autodigestion followed by an inflammation reaction. 80-85% of the patients present with clinically mild (interstitial or edematous), whereas 15-20% of the patients present with a clinically severe (hemorrhagic necrotizing) acute pancreatitis.

Acute pancreatitis is, in 80% of the cases, a result of chronic alcohol abuse (alcoholic pancreatitis) or obstructive gallstones (biliary pancreatitis).

Morphologically mild acute pancreatitis show macroscopic punctiform small peripancreatic fat necrosis, whereas severe acute pancreatitis is characterized by large frequently confluent hemorrhagic necroses mostly affecting peripancreatic fat tissue [13].

Patients with acute pancreatitis present with severe and consistent abdominal pain that radiates toward the back, nausea, vomiting, hematemesis, and melena.

To diagnose acute pancreatitis, it is important to exclude other differential diagnoses at first, such as mumps-pancreatitis. For the diagnosis of acute pancreatitis, at least two of the following three criteria must be fulfilled [14]:

- Abdominal pain
- Elevated amylase/lipase levels (threefold increase above normal concentration levels)
- Pathological findings in ultrasound or contrast-enhanced CT

II. Chronic pancreatitis

Chronic pancreatitis is an inflammatory-fibrotic, chronic disease of the pancreas, mostly accompanied by recurrent and/or persistent abdominal pain due to recurrent necrotizing episodes, autoimmune processes, and duct obstruction. It leads to progressive loss of the exocrine and, in most cases also endocrine pancreatic functions [13] [15].

In approximately 80% of the patients with chronic pancreatitis, alcohol abuse is the primary etiological factor [15]. Further causes are autoimmune processes, genetic factors, or mechanical obstruction of the pancreatic duct.

In the early stages of alcohol-related chronic pancreatitis, the fibrosis is often focal, whereas in advanced stages, it is spread over the whole pancreas [13].

Clinically, chronic pancreatitis starts with episodes of acute pancreatitis accompanied by transient pain attacks. In advanced stages, a pervasive, often persistent pain occurs. In the terminal stage, steatorrhea and diabetes are a result of a lack of digestive enzymes and the destruction of islets of Langerhans, respectively. In addition, jaundice can appear when the distal biliary duct is obstructed. Furthermore, pancreatic carcinoma risk is increased [13].

A diagnosis of chronic pancreatitis should be based only on a combination of pathological findings in functional tests (e.g., quantification of pancreatic elastase 1 (E1) in feces) and imaging examinations (x-ray, CT, MRI, ERCP, EUS, and MRCP). Anamnesis (character of the pain symptoms), physical examination (e.g., erythema ab igne), and laboratory parameters (e.g., amylase/lipase, serum calcium, and blood glucose levels) are also part of the diagnosis [15]. Figure 4 represents a PET scan of the whole body using TOF-^{18}F-FDG of a 50-year-old male with chronic active pancreatitis and elevated inflammatory parameters. Figure 5 reveals significantly increased tracer uptake in the pancreatic head and body of the same patient.

Figure 4 TOF-^{18}F-FDG PET MIP whole-body

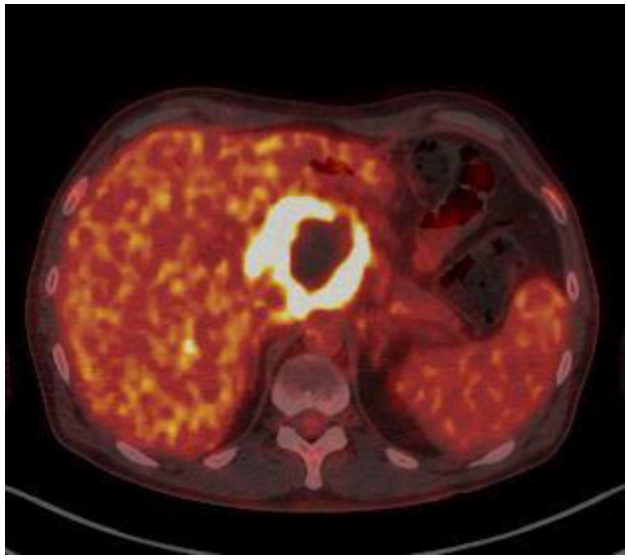

Figure 5 Transaxial PET/CT with TOF

1.2 Imaging techniques of pancreatic diseases

For the medical imaging of pancreatic diseases, many invasive as well as non-invasive examination methods are available. Currently, sectional imaging techniques such as US/EUS, CT, and MRI are in the foreground. However also ^{18}F-FDG PET/CT can be used.

Diagnostic CT of the pancreas

In CT, generally, an iodinated X-ray contrast agent (CA) is injected intravenously. The time delay between CA administration and CT image acquisition is determined by the purpose of the examination [16]. In the case of neoplasms (e.g., benign pancreatic tumors as well as hypervascularized benign and malignant NETs), they are detected in the arterial phase (15-25 seconds after injecting the CA) [17]. In the parenchymal phase (approx. 25-35 seconds post injectionem (p.i.)), the pancreatic tissue shows the highest accumulation of the contrast agent. Hence, pancreas carcinoma, necroses, pseudocysts, and abscesses can be depicted in this phase [16] [17]. Examinations of acute and chronic pancreatitis are conducted in the parenchymal or portal venous phase (40-60 seconds p.i.) [17].

Prior to the CT examination, the patient should be on an empty stomach for six hours [17]. The oral CA is administered approximately fifteen minutes and instantly before the image acquisition with 300 ml of diluted CA each (e.g., Gastrografin or Micropaque CT as a negative CA). In case of excessively vascularized neoplasms, negative CA (e.g., water, methylcellulose solution, or mannitol solution) are optionally administered.

The reconstruction of CT images takes place in the transverse (axial) plane, whereas the slice thickness ranges between 3 mm and 5 mm.

Figure 6 Diagnostic CT with contrast agent in the portal venous phase

Diagnostic CT belongs to standard procedures in pancreatic diagnostics and is conducted predominantly with intravenous CA administration. Non-contrast CT is rarely used because the pancreas is difficult to distinguish from adjacent anatomical structures. It is only required in case of chronic pancreatitis since non-contrast CT imaging is sufficient in order to diagnose gallstones and pancreatic tissue calcifications resulting from chronic pancreatitis. [16] [17]

1.3 Therapy

The therapy of benign tumors of the pancreas consists of different therapy modalities. Serous cystadenoma is treated conservatively. However, an operation should be conducted when clinical symptoms occur. Surgical resection represents the treatment of choice for a mucinous cystadenoma. First-line treatment for IPMNs is also surgical resection (e.g., total pancreatectomy) as well as yearly follow-up examinations through CT or MRI.

In the case of NETs, surgical resection (e.g., enucleation or resection of pancreas segments in case of insulinomas) or non-surgical treatments (such as systemic-drug therapy and local-interventional techniques) are available [5].

Treating acute pancreatitis comprises basic measurements and therapy (monitoring vital parameters), analgesia, fluid and electrolyte substitution, and thromboprophylaxis. In addition, systemic therapy is required to treat shock, respiratory and or renal failure, and prophylaxis of infection through enteral administration of antibiotics [14].

The treatment of patients with chronic pancreatitis includes conservative, interventional, and surgical therapy. Conservative therapy encompasses analgetic medication, (lifelong) abstinence from alcohol, pancreatic enzymes substitution, and dietary measurements, whereas interventional (often endoscopic) therapy is indicated in case of pseudocysts, pancreatic or biliary duct stenosis. Indications for a surgical therapy (e.g., pancreaticojejunostomy) of chronic pancreatitis may include non-manageable pain and suspected pancreatic carcinoma [15].

2 Material and Methods

2.1 Study population

This retrospective study includes a total number of 31 patients (consisting of 19 males and 12 females). This case number of 31 patients was determined by the number of patients with benign pancreatic tumors and conducted TOF-^{18}F-FDG PET/CT and known inflammatory parameters (leukocytes, CRP) at the time of the PET/CT examination of an already completed prospective study.

The mean age of the patients is 60.87 years ranging between 38 and 84 years. The proportion of males in the patients' collective is significantly higher than the proportion of female patients. Hence, there is a skewed gender distribution.

All patients exhibit a histologically confirmed benign tumor of the pancreas (17 solid, 12 cystic and 2 solid-cystic-type tumors). This retrospective study primarily seeks to evaluate the use of the TOF reconstruction algorithm in ^{18}F-FDG-PET/CT in histologically confirmed benign pancreatic lesions.

The patient's data are from the beforementioned completed prospective study from the years 2014-2019 (EK-Nr. 26-040 ex 13/14) and were provided by the Department of Radiology, Division of Nuclear Medicine.

For conducting this study, no written informed consent was mandatory because of the retrospective study design. The local Ethical Committee of the Medical University of Graz approved the study protocol, which was also performed in accordance with the Helsinki Declaration for human studies.

Inclusion criteria in this study are patients with a histologically confirmed benign pancreatic tumor, as well as patients with available inflammatory parameters (leukocytes, CRP) and a blood glucose level less the 160 mg/dl at the time of the PET/CT examination, whereas exclusion criteria are patients without histology/cytology and patients without available inflammatory parameters (leukocytes and CRP) and a blood glucose level greater than 160 mg/dl at the time of the PET/CT examination. Additionally, if available the necrosis factor (LDH) and pancreatic parameters (serum amylase, lipase) were evaluated.

In three out of the 31 patients, no TOF-reconstruction was conducted in early imaging due to a technical defect.

Furthermore, the parameter LDH was not known in four patients and the parameters lipase and amylase were not known in three patients at the time of the PET/CT examination.
Two out of the 31 patients included in this retrospective study had a history of diabetes mellitus (non-insulin-dependent diabetes mellitus), whereas 10 out of the 31 patients showed a history of pancreatitis.

2.2 The concept of radioactive tracers

In nuclear medical diagnostics, radiopharmaceuticals are employed to examine the function of organs and display metabolic processes in the human body. The so-called radiopharmaceuticals (tracer) are chemical substances that are attached with radionuclides. The chemical substances bind specifically to molecular targets (receptors or enzymes) or are metabolized by it [18]. The radiation emitted by these radionuclides is detected then by proper measurement systems. In the in-vivo diagnostics tracers are administered in small quantities into the human metabolism. Thus, a graphical depiction of activity distribution measured in the body is possible (scintigram). Particularly, with tomographic scintigraphies (SPECT, PET), pathological changes can be localized [16].

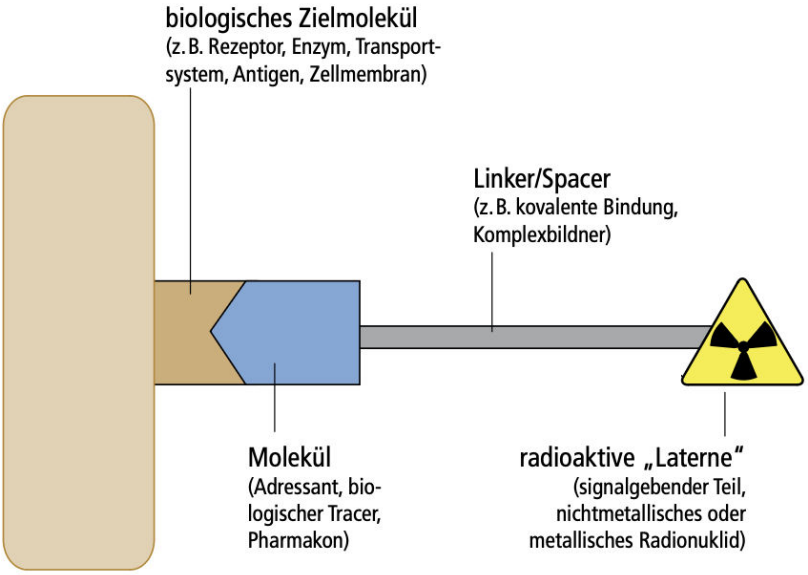

Figure 7 Concept of radioactive tracer [19]

2.3 ^{18}F production

The radionuclide ^{18}F used for labeling FDG is synthesized in a cyclotron, in which stable isotopes (e.g., ^{18}O or ^{20}Ne) are bombarded with charged corpuscles with proper kinetic energy (e.g. < 20 MeV for protons and < 10 MeV for deuterons). By bombarding ^{18}O-enriched water, radionuclide ^{18}F-fluorine is produced in order to synthesize the radiopharmaceutical ^{18}F-FDG [20].

^{18}Fluor represents currently the clinically most important positron emitter for the PET scans. In 2008 over 90% of the clinical studies in Europe were conducted with ^{18}F labeled radiopharmaceuticals. This is due to its excellent nuclide properties, which are, for instance, the low positron energy, which allows a high spatial resolution as well as a low radiation exposure, and its convenient half-life of 109.77 minutes, which allows its transportation to other remote departments [21].

2.4 ^{18}F-FDG

Due to its unique metabolism, ^{18}F-fluordesoxyglucose (2-[^{18}F]FDG or ^{18}F-FDG) represents certainly the most prominent radiopharmaceutical. As a glucose analog, 2-[^{18}F]FDG is transported into the cell through glucose transporters. In the cell a hexokinase irreversibly phosphorylates 2-[^{18}F]FDG. The thus formed 2-[^{18}F]FDG-6-phosphate can no longer exit the cell and is “trapped” in it. In line with this process, the compound accumulates in cells with high metabolism. Owing to the fact that many malignant neoplasms exhibit high rates of glucose metabolism, the radiopharmaceutical 2-[^{18}F]FDG accumulates at higher rates in the neoplasms [22]. The radiolabelled glucose molecules (FDG) cannot undergo further metabolic phosphorylation like the normal glucose molecules since the reaction site of the FDG is labelled with fluorine. This circumstance leads to the accumulation of radioactive and phosphorylated FDG producing a stronger radioactive signal, which can be demonstrated in the PET scan [23].

Figure 8 Whole-body MIP PET scan with physiological distribution pattern of the radiopharmaceutical ^{18}F-FDG

Additionally, attention should be paid to the fact that not only benign and malignant tumors of the pancreas can have a greater tracer-uptake, but also inflammatory pancreatic lesions, due to the higher metabolic rate in these lesions. This results in a diagnostical dilemma differentiating between the various pancreatic lesions when utilizing ^{18}F-FDG PET/CT.

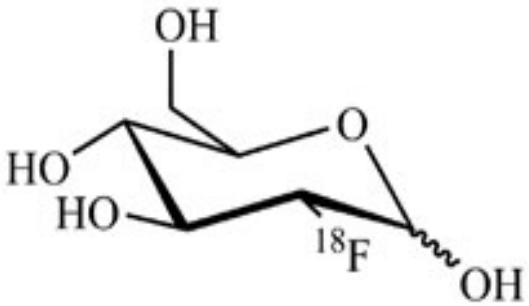

Figure 9 Chemical structure of 2-[^{18}F]-FDG [22]

2.5 The concept of positron emission tomography (PET)

Positron emission tomography (PET) is an imaging technique in nuclear medicine that takes advantage of the $ß^+$ (positron) decay. In this process, positrons are emitted and interact with an electron, which leads to annihilation of the interacting positron and electron (annihilation radiation). Hence, two annihilation photons with a characteristic energy of 511 keV are produced due to this encounter. These photons travel approximately at the velocity of light in diametrically opposed directions towards the detector ring that is located in the tomograph. The oppositely located detectors register the presence of a photon almost simultaneously. Hence, by registering the simultaneous impact of both photons it is possible to locate the annihilation site of the positron-electron-pair [16]. The scintillator material used in the detectors are Bismuth germinate (BGO) and in more modern devices lutetium oxyorthosilicate (LSO), Lutetium yttrium oxyorthosilicate (LYSO) or gadolinium oxyorthosilicate (GSO) [24].

2.6 Time-of-flight

The last years showed an advancement in the technology of PET detectors, which is exclusively available in PET/CT tomographs and not in solely PET detectors. This development applies to the availability of Time-of-flight. This represents a method, which allows a better detection of the tracer distribution along the line-of-response (LOR) through additional measurement of the time difference in detection of the annihilation photons [25]. If the annihilation event lies exactly in the middle of the LOR, then the two annihilation photons would reach the detector elements at the same time. In case the annihilation event takes place elsewhere remote from the middle of the LOR, subsequently one of the two annihilation photons must travel for a shorter period of time than the other photon in order to reach the detector. Fast detectors can measure the time difference between the detection of both annihilation photons. Thus, the location of the annihilation event can be determined along the LOR [26]. In a conventional PET-scan two annihilation photons form the LOR [25]. Thus, the tracer is localized evenly distributed along the LOR. Through TOF-PET the site of the annihilation can be localized (Figure 10 a). This is enabled by measuring the time difference of both annihilation photons (Figure10 b). Figure

10 c shows that TOF-PET enhances the signal-to-noise ratio, which leads to a better image quality of PET scans [25].

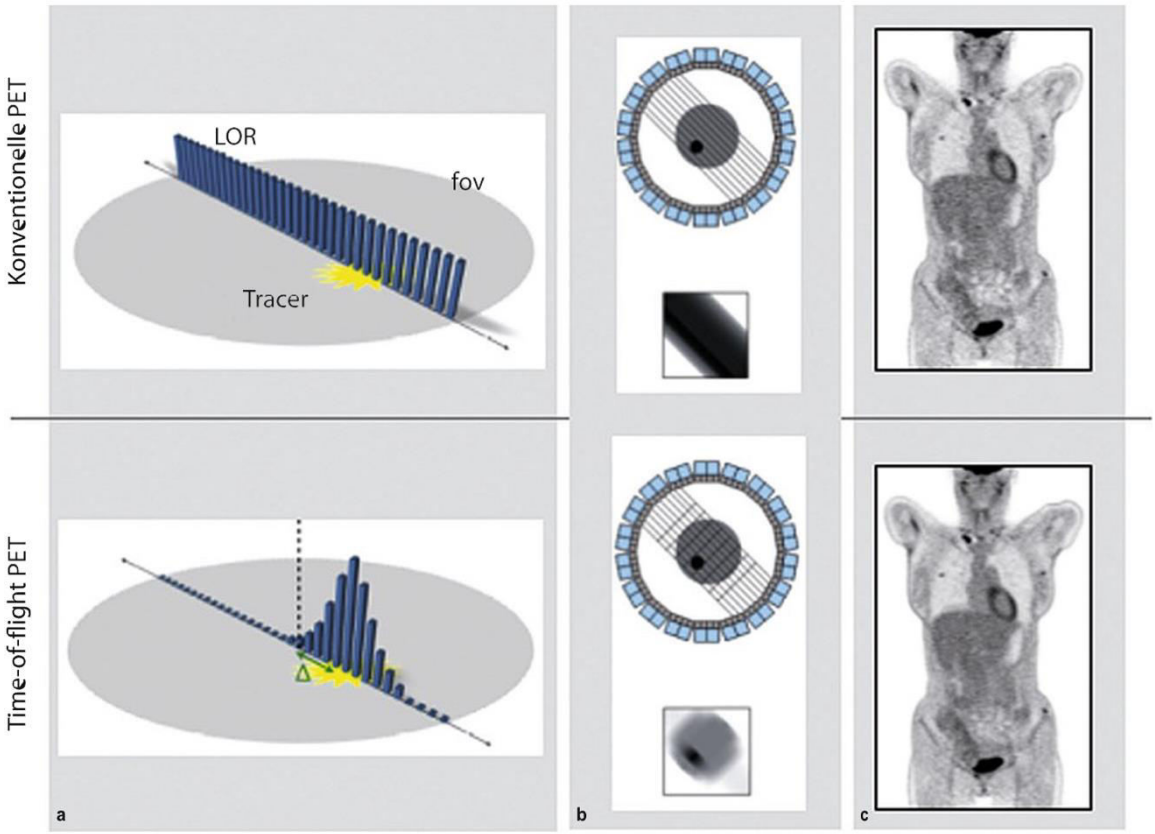

Figure 10 TOF-PET in contrast to non-TOF-PET [25]

TOF-PET has already been discussed in the 1980s und been available commercially since 2006. TOF-PET doesn't result in a higher spatial resolution, but rather in an improvement of the signal-to-noise ratio depending on the object size [25]. In the clinical daily routine TOF-PET can be utilized to reduce the amount of used tracer or to shorten the scan periods [27].

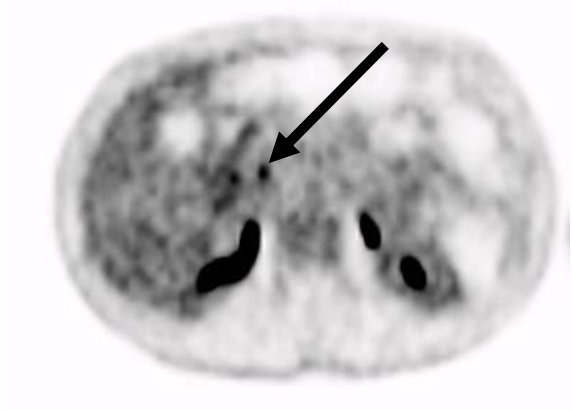

Figure 11 Transaxial PET scan with TOF

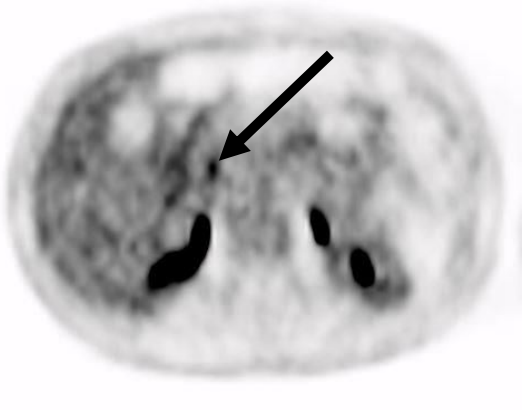

Figure 12 Transaxial PET scan without TOF

Figures 11 represents a transaxial PET scan with TOF, which shows a focal lesion of chronic pancreatitis in the pancreatic head (arrow) in a 46-year-old patient. Figure 12 shows the PET scan for the same patient without TOF.

2.7 Performance of the PET scans

The PET/CT scans consist of early and late scans with and without TOF, respectively. The early scan is a whole-body scan reaching from the base of the scull to the proximal femur, conducted 30 minutes after the intravenous administration of the radiopharmaceutical ^{18}F-FDG, whereas the late scan of the abdomen took place 90 minutes p.i.

The Biograph^{TM}mCT (Siemens Healthineers) and the GE Discovery MI (GE Healthcare Company) were the utilized PET/CT scanners for this purpose. In addition to the early scan an abdominal diagnostic CT with iodine-based contrast agents was conducted 30 minutes after the intravenous administration of ^{18}F-FDG in order to achieve a better evaluation of the pancreatic lesions. The additional diagnostic abdominal CT was conducted without using CA if patients had elevated serum creatinine or decreased GFR (glomerular filtration rate) or low TSH-levels.

After the intravenous administration of the radiopharmaceutical all patients drank 0,5L of water which serves as a negative CA and dilates the intestines.

For six hours prior to the scans the patients were not allowed to eat any solid foods or drink fluids but water. Immediately before the examination the patients were instructed to empty their bladder and remove all metallic objects from their body.

The dose of ^{18}F-FDG administered depends on the weight of the patients. In this study, the mean dose was 339 MBq (240-432 MBq).

2.8 Evaluation of PET/CT images

Initially the PET/CT images of the patients in the prospective study were evaluated by specialists in nuclear medicine. The retrospective evaluation was made by measuring the maximal standardized uptake value (SUVmax) and the volume of interest (VOI), which was placed over the pancreatic lesions.

The term SUV describes the quantitative value of the tracer accumulation in the body. In case of a uniform distribution of the tracer ^{18}F-FDG in the body, SUV would equal 1, but because the tracer physiologically doesn't have an equal distribution in the body, values between 1 and 2 are considered to be normal for the majority of organs. Values greater than 2 often indicate a pathological finding such as a neoplasm or an inflammation. The SUV is calculated by dividing the radioactivity concentration (Bq/g) and the bodyweight (g) by the administered radioactivity (Bq) [28]:

$$SUV = \frac{radioactivity\ concentration\ (\text{Bq/g}) * body\ weight\ (g)}{administered\ radioactivity\ (Bq)}$$

2.9 Statistics

The anonymized patients' data used in this retrospective study were gathered and entered in a Microsoft®-Office-Excel table. The laboratory parameters (inflammatory parameters (leukocytes and CRP), necrosis factor (LDH), and pancreatic parameters (lipase and amylase)) originate from openMEDOCS. The McNemar-test was used to compare the number of correctly identified benign pancreatic lesion with and without TOF. The WILCOXON test was applied to compare the SUVmax and the lesion volume with and without TOF after excluding normal distribution of the data with the Kolmogorov-Smirnov test. Spearman's correlation analysis was used to correlate laboratory parameters (leukocytes, CRP, amylase, lipase) with the SUVmax.

The software utilized for the statistical analysis was IBM SPSS statistics 27, whereas p was seen as significant for values below 0.05.

3 Results

The primary purpose of this retrospective study is to look at the use of the TOF reconstruction algorithm in the evaluation of histologically confirmed pancreatic lesions in ^{18}F-FDG PET/CT scans in comparison to the standard ^{18}F-FDG PET/CT scans. The secondary goals include evaluating the use of the TOF reconstruction algorithm in ^{18}F-FDG PET/CT scans in comparison with the standard scans particularly for pancreatic lesions that are smaller than 3 cm as well as the analysis of the correlation between SUVmax of the pancreatic lesions and specific laboratory parameters.
Therefor early and delayed ^{18}F-FDG PET/CT scans with and without TOF were gathered and compared with each other.

3.1 Patient characteristics

Thirty-one patients were included in this retrospective study in total, 19 of which were males and 12 were females with an average age of 60,87 years spanning between 38 and 84.
Approximately 32% (n=10) of the 31 patients had a prior pancreatitis history, while 68% (n=21) did not. Additionally, only two patients (6%) have a history of non-insulin-dependent diabetes mellitus.
Further details about the remaining patient characteristics are shown in Table 2.

Table 2 Clinical profile of the patients

Characteristics	**Number (n)**
Total Patients	31
Gender:	
Males	19
Females	12
Mean age in years [range]	60.87 [38-84]
History of pancreatitis:	
Yes	10
No	21
History of diabetes mellitus:	
Yes (non-insulin-dependent diabetes mellitus)	2
No	29
Tumor type:	
Solid	17
Cystic	12
Solid-cystic	2
Localization:	
Head	15
Body	9
Tail	2
Uncinated process	5
Histopathological diagnosis	10
no indication of malignancy	
acute pancreatitis	3
chronic pancreatitis	10
MCN with focal low-grade dysplasia)	1
IPMN with intermediate-grad dysplasia (borderline neoplasm)	2
serous microcystic adenoma	4
high-differentiated neuroendocrine tumor (NET)	1
Average lesion size in cm [range]	2.71 [0-10.8]

3.2 Visual imaging assessment in all lesions:

Comparing between the PET/CT scans of the 31 patients with and without the reconstruction algorithm TOF reveals a total diagnostic improvement (of both early and delayed scans) of 16.13% (5/31), whereas in early imaging the improvement was 14.29% and 9.68% in delayed imaging. This improvement comes into existence since the effectivity (correctly as benign identified lesions regarding nonassessable lesions as false negative) with TOF was 58.06 % (18/31) compared to 41.94% (13/31) without TOF (p= 0.112). The sensitivity was 70.97% (22/31) with TOF and 74.19% (23/31) without TOF (p= 1.00) regarding nonassessable lesions as true positive.

Out of the 31 scans 10 were not assessable without TOF, whereas only 4 lesions were not assessable using TOF.

Furthermore, the results of correctly as benign identified lesions in early and delayed scans with and without TOF are listed in Table 3.

The extent of improvement in the diagnostic accuracy of TOF versus standard imaging in diagnosing benign pancreatic lesions is shown in percentage in the column labeled "Diagnostic improvement".

Table 3 Results of visual imaging assessment (n=31)

	TOF	**non-TOF**	**Diagnostic improvement**
Total results	18	13	5/31 (16.13 %)
Early imaging	19*	15**	4/28 (14.29%)
Delayed imaging	16	13	3/31 (9.68%)

*for three patients, early PET/CT scans with TOF were not conducted

**To be able to compare the results of the early imaging without and with TOF, three early scans without TOF were excluded of the same patients because the images with TOF were not available due to a technical defect

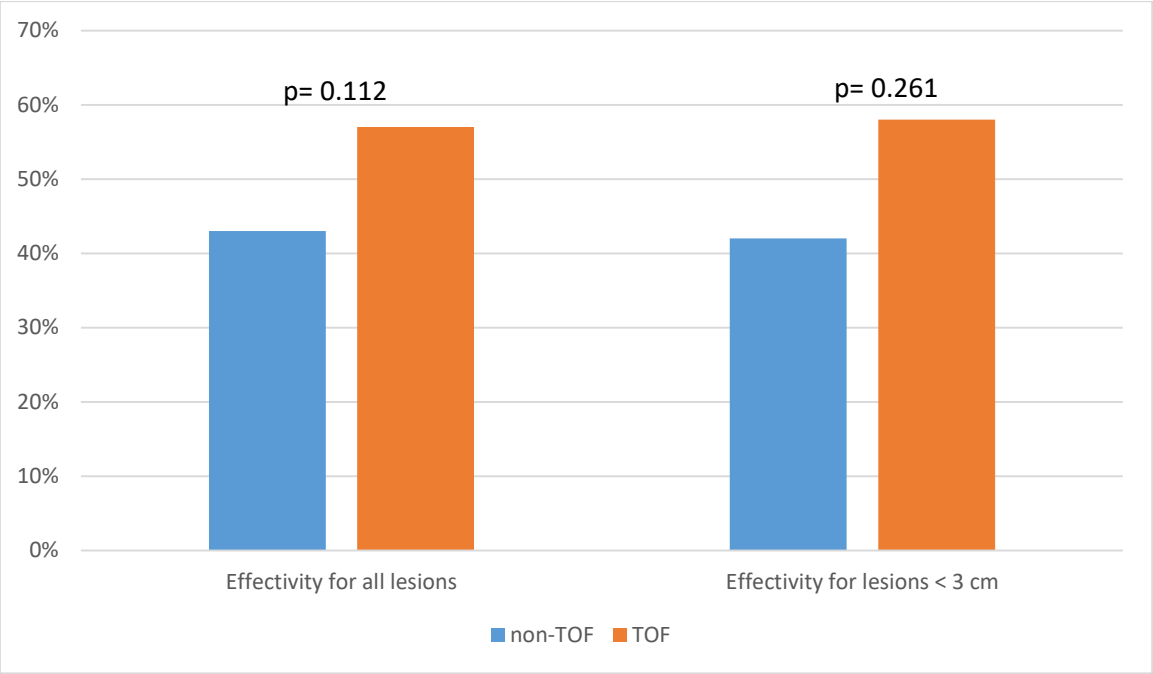

Figure 13 Effectivity with and without TOF for all lesions and lesins < 3 cm

3.3 Visual imaging assessment in lesions smaller than 3 cm:

The size of the 31 lesions averaged 2.71 ± 2.37 cm, with 21 out of the 31 lesions measuring less than 3 cm. With TOF the number of lesions detected as benign was 12 (57.14%) versus 9 (42.86%) without TOF, resulting in a total diagnostic improvement of 14.29% for lesions smaller than 3 cm. In early imaging with TOF 13 lesions were identified as benign versus 11 without TOF. In delayed imaging with and without TOF 10 and 9 lesions were detected as benign, respectively. The findings are summarized in Table 4.

Consequently, the effectivity (regarding nonassessable lesions as false negative) with and without TOF was 57.14% and 42.86% (p= 0.261), respectively. By contrast, the sensitivity came to 71.43% (15/21) and 76.19% (16/21) with and without TOF (p= 1.00), respectively, regarding nonassessable lesions as true positive. Three out of the 21 lesions were not assessable with TOF versus seven without TOF.

Table 4 Results lesions < 3 cm (n=21)

	TOF	**non-TOF**	**Diagnostic improvement**
Total results	12	9	3/21 (14.29%)
Early scans	13	11	2/21 (9.52%)
Delayed scans	10	9	1/21 (4.76%)

3.4 SUVmax in early and delayed imaging and lesion volume in delayed imaging

The average maximal tracer uptake (SUVmax) in the early imaging incorporating TOF-reconstruction was significantly higher compared with early imaging without TOF (4.34 vs. 3.88; $p = 0.002$). This higher maximal tracer uptake was also observed in the delayed imaging with TOF as opposed to non-TOF imaging (4.87 vs. 4.31; $p < 0.001$). With TOF the average lesion volume in delayed imaging was greater than without TOF (34.55 cm^3 vs. 33.86 cm^3). However, the difference was not statistically significant ($p = 0.26$). The results of the comparison of SUVmax and lesion volume are shown in Table 5.

Table 5 Comparison of SUVmax and lesion volume with and without TOF

	With TOF	**non-TOF**	**p**
SUVmax early scan (mean ± SD)	4.34 (± 3.31)	3.88 (± 3.81)	0.002
SUVmax delayed scan (mean ± SD)	4.87 (± 4.71)	4.31 (± 4.51)	<0.001
Volume in cm^3 delayed scan (mean ± SD)	34.55 (± 101.36)	33.86 (± 101.37)	0.26

By comparing the findings of the tracer uptake of the pancreatic lesions in early and delayed imaging with TOF, an increase in the maximal tracer uptake can be noticed in 64.49% of the patients (in 18 out of 28 (due to a technical defect early scans with TOF weren't performed in three patients)). In Contrast, the increase in the maximal tracer uptake in delayed imaging compared to early imaging without TOF was observed in 64.52% of the patients (in 20 out of 31). The increase in the SUVmax in delayed scans compared to early scans was with and without TOF-reconstruction not statistically significant ($p = 0.05$ with TOF; $p = 0.032$ without TOF). The results of semi-quantitative assessment in early and delayed imaging are displayed in Table 6.

Table 6 Results of semi-quantitative assessment in early and delayed imaging

	SUVmax in early scans	**SUVmax in delayed scans**	**p**
TOF (mean ± SD)	4.34 (± 3.31)	4.87 (± 4.71)	0.05
Non-TOF (mean ± SD)	3.88 (± 2.81)	4.31 (± 4.51)	0.032

3.5 Correlation analysis with laboratory parameters

Table 7 displays the information on the average values and standard deviations for the five laboratory parameters evaluated in the study. It is worth noting that the average CRP (c-reactive protein) values exhibited an elevation when compared to the normal reference values.

Table 7 Mean laboratory parameters of the study population

	Leukocytes (G/l)	**CRP (mg/l)**	**Amylase (U/l)**	**Lipase (U/l)**	**LDH (U/l)**
Normal reference values [29]	3.8-10	< 5	28-100	13-60	< 250
Mean (± SD)	**7.18** (± 2.60)	**13.99** (± 15.22)	**42.64** (± 36.3)	**53** (± 45.53)	**204.07** (±97.15)
Range	2.63-13.77	0.4-68.3	5-148	6-222	131-620

To examine the associations between all five laboratory parameters (leukocytes, CRP, amylase, lipase, and LDH) and SUVmax with and without TOF-reconstruction in early and delayed imaging, Spearman's correlation analysis was employed.

As presented in Table 8 below, a statistically significant correlation was detected between amylase values and solely the SUVmax in early imaging with TOF ($p = 0.044$) (Figure 13 (a)). A statistically significant correlation was also spotted between the lipase values and the SUVmax only in early imaging with and without TOF ($p = 0.027$ and $p = 0.037$, respectively) (Figure 14 (a) and Figure 14 (b)), and between CRP and SUVmax in delayed imaging with and without TOF ($p = 0.002$ and $p = 0.001$, respectively) (Figure 15 (a) and (b)). Between amylase and SUVmax in early scans without TOF (Figure 13 (b)) and delayed scans with and without TOF and between the other laboratory parameters (leukocytes and LDH) and SUVmax in both early and delayed scans with and without TOF (Figure 16), no statistically significant correlation was observed.

Table 8 Correlation of laboratory parameters with SUVmax in early and delayed imaging with and without TOF

	SUVmax early scans with TOF*	**SUVmax early scans without TOF**	**SUVmax delayed scans with TOF**	**SUVmax delayed scans without TOF**
Leukocytes (G/l)	p = 0.537	p = 0.704	p = 0.070	p = 0.079
CRP (mg/l)	p = 0.866	p = 0.866	**p = 0.002**	**p = 0.001**
Amylase (U/l)	**p = 0.044**	p = 0.063	p = 0.201	p = 0.386
Lipase (U/l)	**p = 0.027**	**p = 0.037**	p = 0.088	p = 0.200
LDH (U/l)	p = 0.327	p = 0.463	p = 0.608	p = 0.759

*due to technical issues in 3 early scans, TOF was performed in only 28 patients

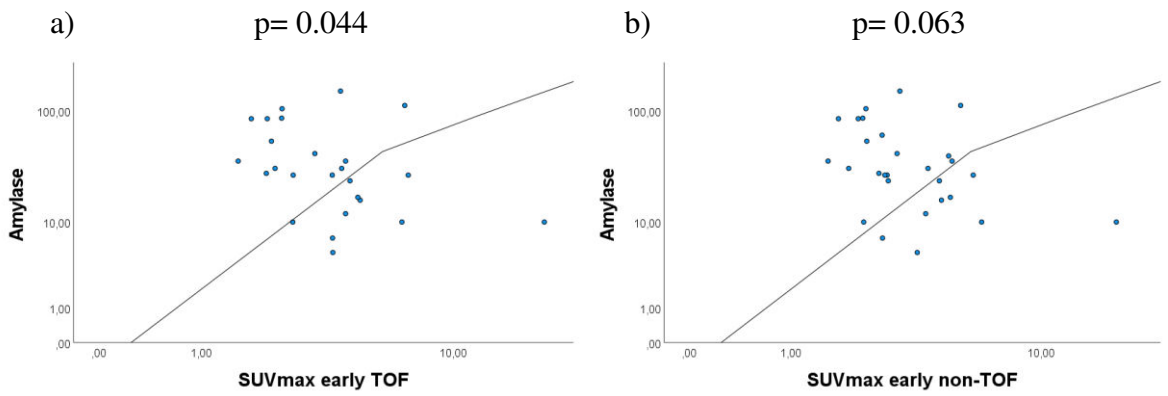

Figure 14 Scatter plots of the correlation between amylase and SUVmax in early imaging with TOF (a) and without TOF (b)

The scatter plots in Figure 14 show a statistically significant correlation between SUVmax in early imaging with TOF and amylase (a) and no statistically significant correlation between SUVmax in early imaging without TOF and amylase (b).

a) p= 0.027 b) p= 0.037

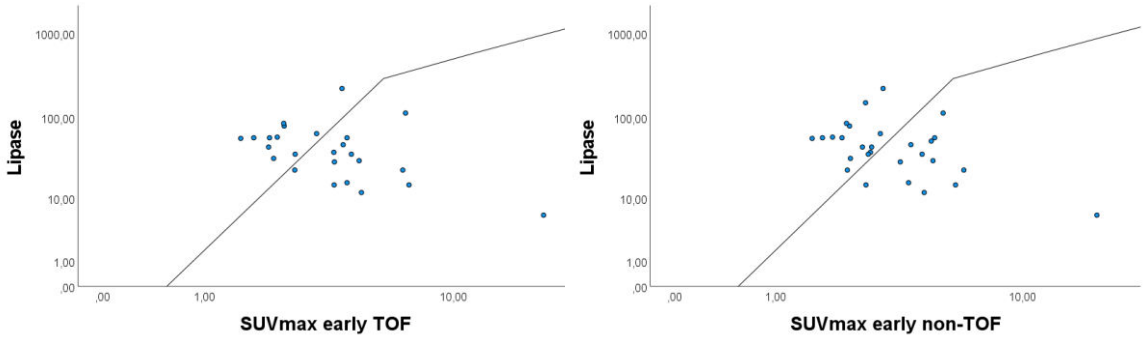

Figure 15 Scatter plots of the correlation between lipase and SUVmax in early imaging with TOF (a) and without TOF (b)

The scatter plots in Figure 15 show a statistically significant correlation between SUVmax in early imaging with (a) and without TOF (b) and lipase.

a) p= 0.002 b) p= 0.001

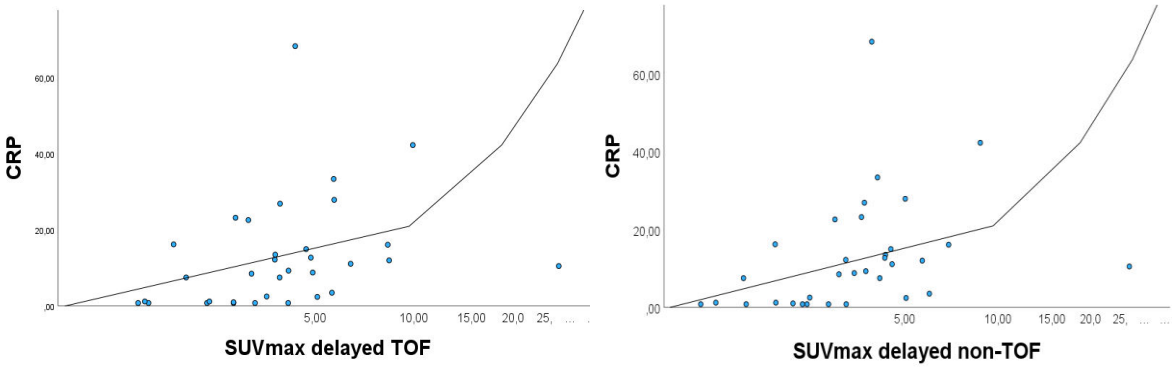

Figure 16 Scatter plots of the correlation between CRP and SUVmax in delayed imaging with TOF (a) and without TOF (b)

The scatter plots in Figure 16 show a statistically significant correlation between SUVmax in delayed imaging with (a) and without TOF (b) and CRP

a) p= 0.070 b) p= 0.079

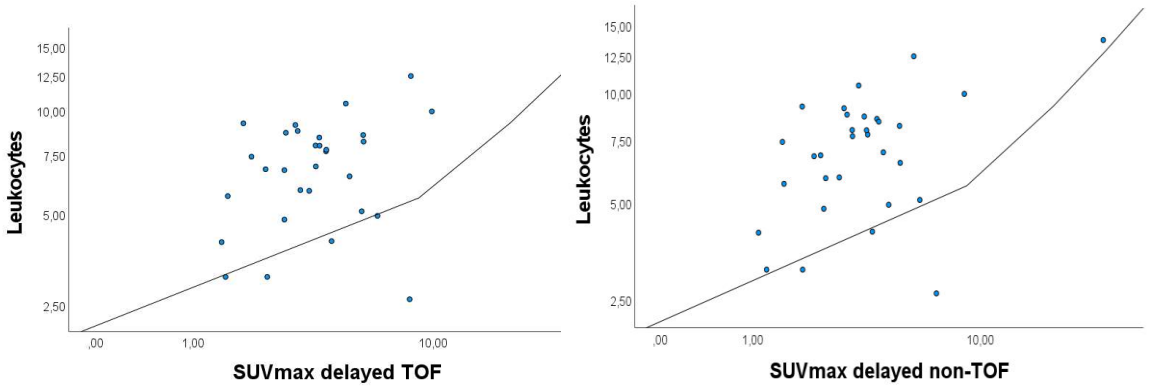

Figure 17 Scatter plots of the correlation between leukocytes and SUVmax in delayed imaging with TOF (a) and without TOF (b)

The scatter plots in Figure 17 show no statistically significant correlation between SUVmax in delayed imaging with (a) and without TOF (b) and leukocytes.

4 Discussion

As an answer to the research question on whether the reconstruction algorithm time-of-flight in ^{18}F-FDG PET/CT improves the diagnostic rate in patients with histologically confirmed benign pancreatic lesions, there was indeed an increase in the number of correctly identified as benign, especially small lesions (< 3 cm). However, no statistically significant improvement was achieved. The analyzed study population consisted of 31 patients with a subgroup of patients with tumor lesions smaller than 3 cm (n= 21).

Out of the 31 scans 10 were not assessable without TOF, whereas only 4 lesions were not assessable using TOF, thus a higher assessability with TOF. Using the reconstruction algorithm 5 out of 31 lesions more were correctly identified compared to the scans not using TOF (18/31 compared to 13/31, respectively). In patients with lesions smaller than 3 cm, the number of lesions detected as benign was 12 with TOF versus 9 without TOF.

The average maximal tracer uptake (SUVmax) in the early and delayed imaging incorporating TOF-reconstruction was significantly higher compared with early and delayed imaging without TOF.

Interestingly, SUVmax increased in delayed scans with and without TOF (Table 6), a typical finding in malignant but not in benign pancreatic tumors, where a decrease in tracer uptake is usually expected.

Shreve PD analyzed in his study the focal ^{18}F-FDG uptake and accumulation in PET scans in inflammatory pancreatic conditions. In 12 out of the 42 involved patients, the focal FDG uptake was due to the inflammation process in the pancreas rather than underlying tumor, as verified by surgical procedures, biopsies, and follow-up assessments. The study involved 42 male patients with an age ranging from 40 to 78 years. In contrast to this current study, where the imaging was conducted 30 and 90 min p.i., the scans in the study of Shreve PD were performed 50-60 min after administering ^{18}F-FDG [30].

He also concluded that inflammatory processes in the pancreas can lead to a higher ^{18}F-FDG uptake similarly to pancreatic tumors [30]. This finding could also be confirmed in the current study in Figure 5, that shows significantly increased tracer uptake in the pancreatic head and body in a patient with chronic active pancreatitis and elevated inflammatory parameters.

Regarding the correlation between SUVmax and laboratory parameters (CRP, leukocytes, amylase, lipase, and LDH) a statistically significant correlation was spotted between amylase values and SUVmax in early imaging with TOF, between lipase values and

SUVmax in early scans with and without TOF, as well as between CRP and SUVmax in delayed scans with and without TOF. Between amylase and SUVmax in early scans without TOF and delayed scans with and without TOF and between the other laboratory parameters (leukocytes and LDH) and SUVmax in both early and delayed scans with and without TOF, no statistically significant correlation was detected. In comparison, in the study of Shreve PD 9 out of 12 patients with increased focal FDG-uptake in the pancreas showed normal leukocyte values, whereas 6 out of 12 showed normal amylase and lipase values [30].
The present study represents the first study in the literature that investigated the correlation between SUVmax and laboratory parameters (CRP, leukocytes, amylase, lipase and LDH) for benign pancreatic lesions in ^{18}F-FDG PET/CT.

Diederichs et al. [31] didn't perform a correlation analysis in their study. They analyzed the diagnostic value of ^{18}F-FDG PET in distinguishing benign from malignant pancreatic tumors in connection with increased and non-increased CRP levels. For this purpose, they divided the patients into three groups depending on their CRP levels (unknown, normal and increased CRP levels) and compared the sensitivity for these groups. They came to the conclusion that false positive results occurred increasingly for patients with raised CRP levels. They stated that elevated CRP levels should be taken into consideration when interpreting ^{18}F-FDG PET scans and signalized the importance of proper selection of the study population to avoid a diagnostic inaccuracy [31].

In another study, Nitzsche et al. [32] performed a dynamic kinetic analysis of ^{18}F-FDG PET to examine whether it can differentiate more precisely between benign and malignant pancreatic lesions than semiquantitative analysis. The study involved 30 patients divided into 4 different groups (control, acute pancreatitis, chronic pancreatitis and pancreatic cancer) who underwent dynamic ^{18}F-FDG PET scans over 90 minutes with the corresponding laboratory parameters specified for each group. They concluded that dynamic kinetic analysis of ^{18}F-FDG PET is more accurate in distinguishing benign from malignant pancreatic lesions compared to semiquantitative uptake value analysis [32].

As an answer to the study above from Shreve PD, Zimny et al. inferred in their Letters to the editor that patients with elevated inflammatory parameters should be excluded from

^{18}F-FDG PET/CT, since it's not possible to differentiate between benign and malignant pancreatic lesions in case of elevated inflammatory parameters [33].
They also mentioned the study from Nitzsche et al. regarding the reduction of false-positive results when performing a dynamic kinetic analysis of FDG PET over 90 minutes [32][33]. On this matter, it should be noted that in clinical practice, dynamic scans over a period of 90 minutes are not practical despite yielding fewer false-positive results.

In their prospective study, Santhosh et al. concluded that performing a dual-phase ^{18}F-FDG PET/CT didn't yield a prognostic value regarding the distinguishing of malignant and benign pancreatic tumors. However conducting delayed imaging can provide valuable information about the prognosis, which can contribute to a better therapy regime [34].

Another study from Kawada et al. found that conducting a dual-phase FDG PET/CT can provide a better diagnostic accuracy regarding small pancreatic lesions (< 25 mm) compared to single-phase FDG PET/CT. The study also showed that the increase of tracer uptake (SUVmax) in delayed scans was higher in malignant lesions than in benign lesions smaller than 25 mm [35].

5 Conclusion

Differentiating between inflammatory lesions of the pancreas and pancreatic tumors represents a diagnostic challenge, which this work aims to illustrate. Our study demonstrated that with the use of TOF reconstruction, there was an improvement of 16.1% in the diagnostic rate compared to standard ^{18}F-FDG PET/CT scans without TOF. Although no statistically significant improvement in the diagnosis rate was achieved, more and particularly small (< 3 cm) lesions could be identified as benign.
A significant correlation was also found between the laboratory parameters amylase, lipase and CRP and the SUVmax.

6 References

[1] Schünke M, Schulte E, Schumacher U, et al. Prometheus Lernatlas der Anatomie: Innere Organe. 6th fully revised ed. Stuttgart: Thieme; 2022. p. 278-279.

[2] Aumüller G, Aust G, Engele J, et al. Duale Reihe Anatomie. 5th corrected ed. Stuttgart: Thieme; 2020. p. 748-756.

[3] WHO Classification of Tumours Editorial Board. Digestive system tumours [Internet]. Lyon (France): International Agency for Research on Cancer; 2019 [cited 2022 Dec 01]. (WHO classification of tumours series, 5th ed.; vol. 1). Available from: https://tumourclassification.iarc.who.int/chapters/31.

[4] Dominguez-Munoz JE. Clinical Pancreatology for Practising Gastroenterologists and Surgeons. 2nd ed. Newark: John Wiley & Sons, Incorporated; 2021. p. 577-578.

[5] Ringel J, Mayerle M, Lerch MM. Pankreastumoren. In: Messmann H, editor. Klinische Gastroenterologie: Das Buch für Fort- und Weiterbildung plus DVD mit über 1400 Befunden. Stuttgart: Thieme; 2012. p. 743-749.

[6] Gill A, Singhi A, Adsay N, et al. Serous neoplasms of the pancreas. In: WHO Classification of Tumours Editorial Board. Digestive system tumours [Internet]. Lyon (France): International Agency for Research on Cancer; 2019 [cited 2022 Dec 01 (WHO classification of tumours series, 5th ed.; vol. 1). Available from https://tumourclassification.iarc.who.int/chaptercontent/31/118

[7] King-yin Lam A, Klöppel G, Klimstra D, et al. Pancreatic neuroendocrine neoplasma: Introduction. In: WHO Classification of Tumours Editorial Board. Digestive system tumours [Internet]. Lyon (France): International Agency for Research on Cancer; 2019 [cited 2022 Dec 01 (WHO classification of tumours series, 5th ed.; vol. 1). Available from https://tumourclassification.iarc.who.int/chaptercontent/31/276

[8] King-yin Lam A, Perren A, Singhi A, et al. Insulinoma. In: WHO Classification of Tumours Editorial Board. Digestive system tumours [Internet]. Lyon (France): International Agency for Research on Cancer; 2019 [cited 2022 Dec 01 (WHO classification of tumours series, 5th ed.; vol. 1). Available from https://tumourclassification.iarc.who.int/chaptercontent/31/148

[9] King-yin Lam A, Kasajima A, Courvelard A, et al. Gastrinoma. In: WHO Classification of Tumours Editorial Board. Digestive system tumours [Internet]. Lyon (France): International Agency for Research on Cancer; 2019 [cited 2022 Dec 01 (WHO classification of tumours series, 5th ed.; vol. 1). Available from https://tumourclassification.iarc.who.int/chaptercontent/31/151

[10] King-yin Lam A, Klöppel G, Klimstra D, et al. Non-functioning pancreatic neuroendocrine tumours. In: WHO Classification of Tumours Editorial Board. Digestive system tumours [Internet]. Lyon (France): International Agency for Research on Cancer; 2019 [cited 2022 Dec 01 (WHO classification of tumours series, 5th ed.; vol. 1). Available from https://tumourclassification.iarc.who.int/chaptercontent/31/147

[11] Klimstra D, Basturk O, Esposito I, et al. Pancreatic mucinous cystic neoplasm. In: WHO Classification of Tumours Editorial Board. Digestive system tumours [Internet]. Lyon (France): International Agency for Research on Cancer; 2019 [cited 2022 Dec 01 (WHO classification of tumours series, 5th ed.; vol. 1). Available from https://tumourclassification.iarc.who.int/chaptercontent/31/124

[12] Riede U, Werner M. Allgemeine und spezielle Pathologie. 2nd ed. Berlin: Springer; 2017. p. 561-561.

[13] Agaimy A, Höfler G, Kreipe H H. Pathologie: Das Lehrbuch. 6th ed. München: Elsevier; 2019. p. 681-684.

[14] Lankisch PG. Akute Pankreatitis. In: Messmann H, editor. Klinische Gastroenterologie: Das Buch für Fort- und Weiterbildung plus DVD mit über 1400 Befunden. Stuttgart: Thieme; 2012. p. 713-721.

[15] Lankisch PG. Chronische Pankreatitis. In: Messmann H, editor. Klinische Gastroenterologie: Das Buch für Fort- und Weiterbildung plus DVD mit über 1400 Befunden. Stuttgart: Thieme; 2012. p. 727-733.

[16] Reiser M, Kuhn FP, Debus J. Radiologie. 4th ed. Stuttgart: Thieme; 2017.

[17] Prokop M, Galanski M, Engelke C. Ganzkörper-Computertomographie: Spiral- und Multislice-CT. 2nd ed. Stuttgart: Thieme; 2007.

[18] Neumaier B. Tracer-Prinzip. In: Dietlein M, Kopka K, Schmidt M, editors. Nuklearmedizin: Basiswissen und klinische Anwendung. 8th ed. Stuttgart: Schattauer; 2017. p. 12-13.

[19] Schicha H, Schober O. Nuklearmedizin: Basiswissen und klinische Anwendung. 7th fully revised and expanded ed. Stuttgart: Schattauer; 2013. p. 36-36.

[20] Kopka K, Wagner S. Radionuklidproduktion. In: Dietlein M, Kopka K, Schmidt M, editors. Nuklearmedizin: Basiswissen und klinische Anwendung. 8th ed. Stuttgart: Schattauer; 2017. p. 76-76.

[21] Rösch F, Piel M. Radiochemie/Tracer. In: Mohnike W, Hör G, Schelbert H, editors. PET/CT-Atlas: Interdisziplinäre onkologische, neurologische und kardiologische PET/CT-Diagnostik. 2nd ed. Berlin, Heidelberg: Springer; 2011. p. 47-48.

[22] Rösch F, Piel M. Radiochemie/Tracer. In: Mohnike W, Hör G, Schelbert H, editors. PET/CT-Atlas: Interdisziplinäre onkologische, neurologische und kardiologische PET/CT-Diagnostik. 2nd ed. Berlin, Heidelberg: Springer; 2011. p. 62-63.

[23] Zimmermann R, Couchot P. Nuclear medicine: radioactivity for diagnosis and therapy. 2nd ed. Les Ulis: EDP sciences; 2017. p. 101-101.

[24] Stegger L, Eschner W. Emissionstomographie mit Postironenstrahlern (PET). In: Dietlein M, Kopka K, Schmidt M, editors. Nuklearmedizin: Basiswissen und klinische Anwendung. 8th ed. Stuttgart: Schattauer; 2017. p. 96-96.

[25] Beyer T. Physik/Technik. In: Mohnike W, Hör G, Schelbert H, editors. PET/CT-Atlas: Interdisziplinäre onkologische, neurologische und kardiologische PET/CT-Diagnostik. 2nd ed. Berlin, Heidelberg: Springer; 2011. p. 21-23.

[26] Kadrmas DJ, Casey ME, Conti M. Impact of time-of-flight on PET tumor detection. J Nucl Med. 2009;50:1315-1323.

[27] Murray I, Kalemis A, Glennon J, et al. Time-of-flight PET/CT using low-activity protocols: potential implications for cancer therapy monitoring. Eur J Nucl Med Mol Imaging. 2010;37:1643-1653.

[28] Stegger L, Eschner W. Bildverarbeitung und Kommunikation. In: Dietlein M, Kopka K, Schmidt M, editors. Nuklearmedizin: Basiswissen und klinische Anwendung. 8th ed. Stuttgart: Schattauer; 2017. p. 105-106.

[29] Herold G. Innere Medizin. Köln: Gerd Herold; 2023. p. 967-973.

[30] Shreve PD. Focal fluorine-18 fluorodeoxyglucose accumulation in inflammatory pancreatic disease. Eur J Nucl Med. 1998;25(3):259-264.

[31] Diederichs CG, Staib L, Glasbrenner B, et al. F-18 Fluorodeoxyglucose (FDG) and C-Reactive Protein (CRP). Clin Positron Imaging. 1999;2(3):131-136.

[32] Nitzsche EU, Hoegerle S, Mix M, et al. Non-invasive differentiation of pancreatic lesions: is analysis of FDG kinetics superior to semiquantitative uptake value analysis? Eur J Nucl Med. 2001;29(2):237-242.

[33] Zimny M, Buell U. False-positive FDG PET in patients with pancreatic masses: an issue of proper patient selection? Eur J Nucl Med.1998;25(9):1352-1353.

[34] Santhosh S, Mittal BR, Bhasin D, et al. Dual-phase 18F-FDG PET/CT imaging in the characterization of pancreatic lesions: does it offer prognostic information? Nucl Med Commun. 2014;35(10):1018-1025.

[35] Kawada N, Uehara H, Hosoki T, et al. Usefulness of dual-phase 18F-FDG PET/CT for diagnosing small pancreatic tumors. Pancreas. 2015;44(4):655-659.